Carbohydrate Polymers 87 (2012) 2313–2319

Contents lists available at SciVerse ScienceDirect

Carbohydrate Polymers

journal homepage: www.elsevier.com/locate/carbpol

# Preparation of chitin nanofibril/polycaprolactone nanocomposite from a nonaqueous medium suspension

Ya-li Ji[b,c], Patricia S. Wolfe[a], Isaac A. Rodriguez[a], Gary L. Bowlin[a,*]

[a] Department of Biomedical Engineering, Virginia Commonwealth University, Richmond, VA 23298, USA
[b] State Key Laboratory For Modification of Chemical Fibers and Polymer Materials, Donghua University, Shanghai 201620, China
[c] College of Material Science and Engineering, Donghua University, Shanghai 201620, China

ARTICLE INFO

*Article history:*
Received 27 September 2011
Received in revised form 11 October 2011
Accepted 29 October 2011
Available online 6 November 2011

*Keywords:*
Chitin nanofibril
Nanocomposite
Polycaprolactone
Electrospinning

ABSTRACT

Chitin nanofibrils are prepared by treatment of commercial chitin in hydrochloric acid. It is found for the first time that the obtained chitin nanofibrils can be well dispersed in an organic solvent of 2,2,2-trifluoroethanol (TFE) due to its strong ability to form hydrogen bonds. Polycaprolactone (PCL), a water insoluble biodegradable polymer, is selected to blend with chitin nanofibrils to achieve chitin nanofibril/polycaprolactone (n-chitin/PCL) nanocomposites using TFE as a co-solvent. The results show the n-chitin/PCL nanocomposites, either in the form of solvent-cast films or electrospun fiber mats, both exhibit reinforced mechanical properties. Thus, the processing technique from a TFE suspension instead of aqueous suspensions is a good alternative to broaden the family of chitin nanofibril-based nanocomposites.



## 1. Introduction

Chitin, the second most abundant biopolymer next to cellulose, possesses many favorable properties such as non-toxicity, high crystallinity, biocompatibility and biodegradability. Acid-treatment of chitin can dissolve away regions of low lateral order, resulting in elongated rod-like nanoparticles, termed "nanofibrils" (otherwise called nanowhiskers, or nanocrystals). Beside traditional acid-treatment, there are several other approaches to obtain chitin nanofibrils, such as mechanical treatment or acid-assisted mechanical treatment (Ifuku et al., 2009, 2010), which can achieve a high-aspect-ratio chitin nanofibril, ionic liquid treatment (Kadokawa, Takegawa, Mine, & Prasad, 2011), and TEMPO-mediated oxidation treatment (Fan, Saito, & Isogai, 2008). Muzzarelli (2011a, 2011b, 2011c, 2011d) reviewed the recent advances in chitin nanofibril and its preparation technique in detail. Generally, fresh crustacean shells were treated in the lab to prepare chitin nanofibrils (Muzzarelli, 2011c), because commercial chitin possibly experienced a number of denaturing treatments. But here we still use commercial chitin to prepare chitin nanofibrils due to its convenience to obtain.

Chitin nanofibrils are an emerging, novel nanofiller, and have been shown to bring about reinforcing effects on both synthetic and natural polymeric structures. The good biocompatibility and biodegradability also make it one of the most promising fillers, especially in biomedical field. Since chitin is essentially a good scaffold material that is in favor of cell adhesion and growth, so its acid-treated product, chitin nanofibril, can be both acting as reinforcing nanofiller and bioactive reagent to facilitate scaffold in tissue engineering. However, there is a common viewpoint that nanofibrils only well disperse in aqueous solution, and poorly disperse in organic solvents, which to some extent restricts the development of nanofibril-based nanocomposites with the present processing technique. Generally, there are two routes often used to obtain a good dispersion of the chitin nanofibril fillers within the polymer matrix. One requires the use of either an aqueous suspension of the polymer (Nair & Dufresne, 2003; Paillet & Dufresne, 2001), i.e., latex, or an aqueous solution of the polymer (Hariraksapitak & Supaphol, 2010; Junkasem, Rujiravanit, Grady, & Supaphol, 2010; Lu, Weng, & Zhang, 2004; Mathew, Laborie, & Oksman, 2009; Sriupayo, Supaphol, Blackwell, & Rujiravanit, 2005a, 2005b; Watthanaphanit, Supaphol, Tamura, Tokura, & Rujiravanit, 2008; Wongpanit et al., 2007; Zengab, Gaoa, Wua, Fana, & Li, 2010), i.e., water-soluble polymers. However, the latex approach introduces a large amount of emulsifier or surfactant to the system; water-soluble polymers are only limited to several species. The other requires modification of the chitin nanofibril surface with functional groups or chains to improve its miscibility with organic solvents or matrix polymers. Feng et al. (2009) densely grafted long polycaprolactone (PCL) tails onto the nanofibril surface based on a "graft from" strategy and obtained a bionanocomposite that could be injection-molded as sheets. Fan et al. (2008) tried a TEMPO-mediated oxidation route and obtained carboxylic groups modified chitin nanofibril, aiming to make it easier to

* Corresponding author. Tel.: +1 804 828 2592; fax: +1 804 828 4454.
*E-mail address:* glbowlin@vcu.edu (G.L. Bowlin).

0144-8617/$ – see front matter © 2011 Elsevier Ltd. All rights reserved.
doi:10.1016/j.carbpol.2011.10.066

form ester group or others groups by the reaction of carboxylic groups. But such modifications potentially screen the interaction between chitin nanofibrils and make it difficult to form a desired percolation structure so as to influence the reinforcing effect.

2,2,2-Trifluoroethanol (TFE) is a good solvent for many synthetic polymers. TFE is also miscible with many solvents such as water, alcohol, ketone, benzene, and toluene. More importantly, TFE can promote formation of a secondary structure in polypeptides and proteins, which allows it to be widely employed in biophysical and biotechnological investigation. Most of these effects have been ascribed to the presence of hydrogen-bonds. The high electron-withdrawing ability of the $-CF_3$ group is expected to exhibit a weak acidity (ionization constant of $pK_a = 12.37$). We found that the chitin nanofibril can be well dispersed in TFE assisted by ultrasonic treatment. Thus, it is possible to directly blend chitin nanofibrils with many other water-insoluble polymers to broaden the family of chitin nanofibril-based nanocomposites, especially for preparation of electrospun fibrous nanocomposites. Meanwhile, it provides an investigation platform aiming to unravel the mechanism of chitin nanofibrils reinforcing matrix polymers and elucidate the effects of the affinity between chitin nanofibril and matrix polymer on mechanical behaviors if all kinds of chitin nanofibril-based nanocomposites can be easily prepared. In this paper, TFE was used to blend chitin nanofibrils with a commonly used biodegradable polymer, polycaprolactone (Shalumon et al., 2011) and the preliminary results of the mechanical properties of the nanocomposites were briefly discussed.

## 2. Experimental

### 2.1. Preparation of chitin nanofibrils

Chitin nanofibrils were prepared according to Dufresne's approach with some modification (Paillet & Dufresne, 2001). Briefly, chitin flakes (C9213, Sigma–Aldrich, USA) were treated in 3 N hydrochloric acid (HCl) under stirring and refluxing for 6 h. The ratio of the 3 N HCl solution to chitin was 30 $cm^3\,g^{-1}$. The residue was collected after centrifugation and treated again with 3 N HCl twice. The residue was then washed with deionized water three times by centrifugating and decanting of the supernatant. The obtained suspension was further dialyzed against deionized water at room temperature for 3 days, followed by ultrasonic treatment in a sonicating bath (Whaledent Biosonic, USA) for 20 min and subsequent filtration to remove residual aggregates. Finally, the clear colloidal aqueous suspension was lyophilized to obtain light yellow powders. The yield is about 55%. The reason why we utilized chitin nanofibril powders not chitin nanofibril aqueous suspension was that the powders were easy to accurately weigh and then to be redispersed in solvents.

### 2.2. Preparation of n-chitin/PCL nanocomposite

A desired amount of chitin nanofibril powders were redispersed in deionized water by sonicating for 30 min, followed by solvent-exchanging from water to acetone through centrifugation, and then the pasty chitin nanofibrils were well dispersed in TFE (TCI America Inc., USA) by sonicating for 30 min, finally, a colloidal suspension was obtained; PCL ($M_n = 80\,000\,g\,mol^{-1}$; Fluka, USA) was dissolved in TFE under shaking overnight. The two parts were mixed together and further sonicated for 30 min. A clear mixture was then obtained. The mass ratios of chitin nanofibril filler to PCL were controlled at 5:95, 10:90, 15:85, 20:80, 25:75 and 30:70. To prepare n-chitin/PCL film, the mixture was cast onto a glass petri dish and slowly evaporated at room temperature for 1 day prior to further characterization. To prepare n-chitin/PCL electrospun fiber mats, the mixture was loaded into a 5 $cm^3$ plastic syringe fitted with an 18-gauge blunt-tipped needle, and dispensed at 1 $cm^3\,h^{-1}$ using a syringe pump (KD Scientific, USA). The applied voltage was fixed at 20 kV, the distance between the needle tip and the grounded mandrel (cylindrical, diameter = 2.5 cm) was 15 cm, and mandrel rotation speed was 400 rpm.

### 2.3. Characterization

*Transmission electron microscopy (TEM)*: The chitin nanofibril powders were redispersed either in deionized water or in TFE by sonication. The obtained suspensions were further diluted and cast onto carbon-coated 200-mesh copper grids, slowly evaporated at room temperature, and observed on a JEOL JEM-1230 transmission electron microscope. The images were analyzed by the ImageJ 1.42 software. Electrospun fibers for the TEM analysis was prepared by directly electrospinning n-chitin/PCL mixture onto a carbon-coated 200-mesh copper grid, drying, and then staining by 2% uranyl acetate.

*Scanning electron microscopy (SEM)*: The morphologies of chitin nanofibril powders and section of n-chitin/PCL film (fractured under liquid nitrogen) were observed on a Hitachi SU-70 field emission scanning electron microscope. The electrospun fiber mats were observed on a JEOL JSM-5610LV scanning electron microscope. The images were analyzed by the ImageJ 1.42 software.

Fourier transform infrared (FTIR) spectra were measured (reflection mode) on a Nicolet 670 Nexus FTIR Spectrometer using a Smart iTR Diamond accessory at 4 $cm^{-1}$ resolution.

Wide-angle X-ray diffraction (WAXD) patterns were recorded on a PANalytical X'pert PRO diffractometer operated at 45 kV and 40 mA at room temperature. The scan speed was 3° $min^{-1}$ in the range of 5–50°. The relative crystallinity was calculated using the Jade 6.0 software.

The light transmittance spectra of 0.1% (w/v) chitin nanofibrils in water and in TFE dispersions were measured from 350 to 750 nm using a SpectraMax Plus384 Microplate Spectrometer.

A Nikon Eclipse LV100D-U polarized optical microscope was used to observe the chitin nanofibril dispersions in water and in TFE for evaluating the uniformity of dispersion.

Dynamic mechanical analysis (DMA) was carried out on a TA Rheometrics Solids Analyzer (RSA-III) performing at 1 Hz frequency and a heating rate of 5 °C $min^{-1}$ from −90 °C in a tension mode. The specimens with thickness about 0.2–0.3 mm were cut into 5 mm-wide strips using parallel blade cutter (length setting was 10 mm).

Uniaxial tensile tests were performed on a MTS Bionix 200 Mechanical Testing System instrument (MTS Systems Corp., USA) with a crosshead speed of 100 mm $min^{-1}$. Samples were cut into "dog-bone" shapes by a die punch (narrowest width of 2.67 mm and gage length of 7.49 mm). The results of tensile modulus, peak stress and break at strain were the average of 5 specimens.

## 3. Results and discussion

### 3.1. Fabrication and characterization of chitin nanofibrils

The scanning electron micrograph of lyophilized chitin nanofibril powders is shown in Fig. 1A. The chitin nanofibril powder was composed of chitin fragment meshes. The estimated average width of chitin fragment was 20 nm, but the length was difficult to evaluate due to the crossing and overlapping of the fragments. Fig. 1B shows the transmission electron micrograph of a dilute aqueous suspension obtained by redispersing chitin nanofibril powders into water. The aqueous suspension was constituted of individual chitin fragments consisting of acerose fibrils. The estimated

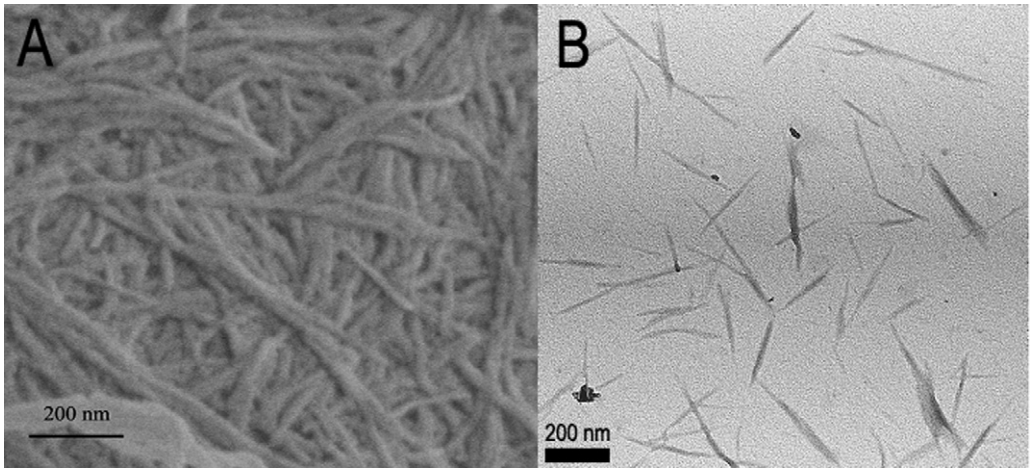


**Fig. 1.** (A) Scanning electron micrograph of the lyophilized chitin nanofibril powders. (B) Transmission electron micrograph of a dilute aqueous suspension of chitin nanofibrils.

average width of chitin fragment was still 20 nm, indicating powders can be well redispersed in water. The estimated average length was 300 nm, thus, the aspect ratio $L/d$ ($L$ being the length and $d$ being the diameter or width) was around 15.

The degrees of deacetylation of original chitin and chitin nanofibril were compared qualitatively based on the ratio of the absorbance of the amide II band at 1560 $cm^{-1}$ to that of the band at 2880 $cm^{-1}$ ($A_{1560}/A_{2880}$) through FTIR spectra according to Sannan's previous work (Sannan, Kurita, Ogura, & Iwakura, 1978) (Fig. S1, Supporting Information). The results showed the ratio of $A_{1560}/A_{2880}$ of chitin nanofibril was nearly the same as that of original chitin, meaning the degrees of deacetylation of original chitin and chitin nanofibril were almost the same, both less than 10%. Thus, the acid-treatment procedure did not significantly affect the degrees of deacetylation of chitin. The FTIR spectra of both chitin and chitin nanofibril in the region of 1660–1620 $cm^{-1}$ (amide I) presented two strong absorption peaks at 1658 and 1622 $cm^{-1}$, indicating a typical α-chitin (β-chitin has only one absorption peak at 1656 $cm^{-1}$) (Cardenas, Cabrera, Taboada, & Miranda, 2004). The absence of the peak at 1540 $cm^{-1}$ (corresponding to the proteins) proved that all the proteins were eliminated from chitin and chitin nanofibril (Gaill, Persson, Sugiyama, Vuong, & Chanzy, 1992). Compared to the work of Muzzarelli et al. (2007), of whom FTIR spectrum was the best so far available for chitin nanofibrils, ours was not so fine as expected. The potential reason may be ascribed to the limitation of acid-treatment approach.

WAXD analysis revealed that there were six main diffraction peaks at ca. 9.2° (0 2 0), ca. 12.6° (0 2 1), ca. 19.1° (1 1 0), ca. 20.7° (1 2 0), ca. 23.6° (1 3 0) and ca. 26.3° (1 3 0) both in original chitin and in chitin nanofibril (Fig. S2, Supporting Information). Careful evaluation of the obtained diffraction patterns by curve-fitting using Jade 6.0 software revealed that the relative crystallinity of chitin nanofibril (76.9%) was slightly greater than that of original chitin (74.0%), which was consistent with our expectation.

### 3.2. Dispersion of chitin nanofibrils in TFE solvent

Fig. 2A shows the transmission electron micrograph of a dilute TFE suspension prepared by redispersing chitin nanofibril powders into TFE. Within the visual field of microscope, individual chitin fragments were uniformly distributed, and the estimated average width and length were the same as in aqueous suspension, indicating TFE a good solvent to disperse chitin nanofibrils.

The light transmittances were wavelength-dependent, which is related to the microfibril widths (Carr & Hermans, 1978; Okita,

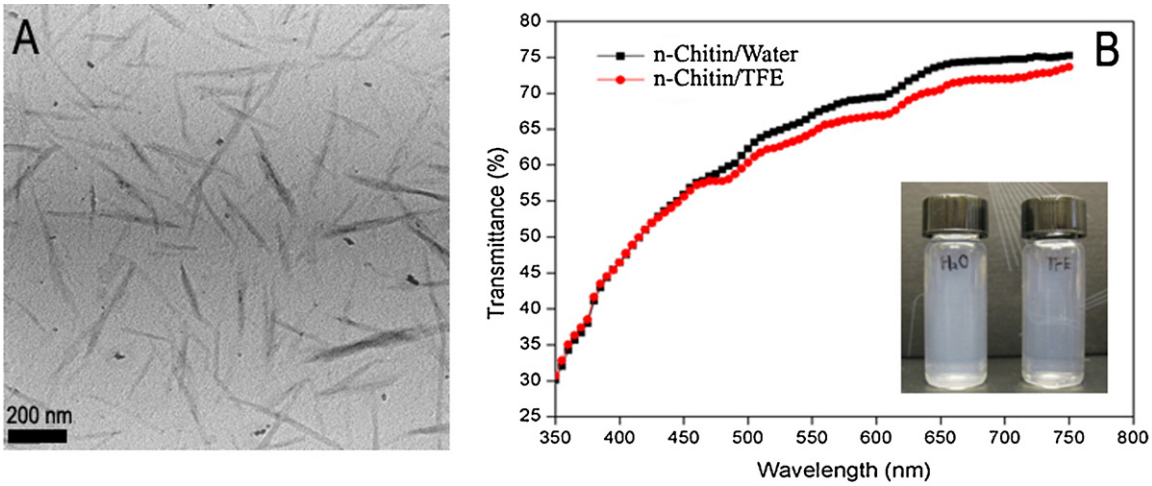


**Fig. 2.** (A) Transmission electron micrograph of a dilute TFE suspension of chitin nanofibrils. (B) Dispersibility of chitin nanofibrils in water and in TFE with the chitin nanofibril content of 0.1% (w/v). Inset is the photo of the corresponding dispersions.

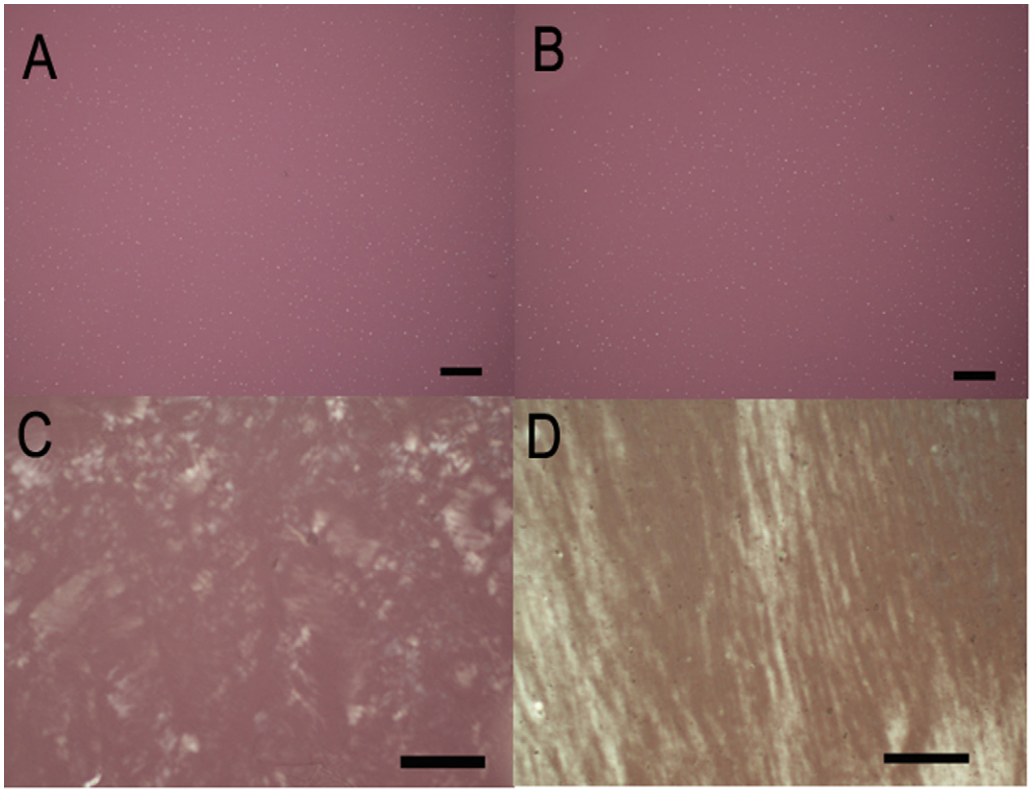


**Fig. 3.** Cross-polarizing optical microphotographs of chitin nanofibril dispersed in water (A and C) and in TFE (B and D) with the chitin nanofibril content of 0.1% (w/v) (A and B) and 5% (w/v) (C and D). Scale bar: 200 μm.

Fujisawa, Saito, & Isoga, 2011). Fig. 2B compares the light transmittance spectra of the chitin nanofibril in water and in TFE dispersions. The transmittance of the chitin nanofibril in TFE dispersion nearly approached that in water dispersion, revealing TFE, just like water, was a good solvent for chitin nanofibrils dispersion. Both suspensions had high transmittances of >65% at 600 nm. The inset is an optical image of corresponding suspensions. It was found that both suspensions were stable at room temperature for more than one week until sedimentation.

Fig. 3 shows the cross-polarizing optical microphotographs of chitin nanofibrils dispersed in water and in TFE. When the chitin nanofibril content was as low as 0.1% (w/v) (Fig. 3A and B), in both cases there appeared a large number of uniformly distributive bright dots representing the birefringence of chitin fragment crystallites, further proving chitin nanofibrils were uniformly dispersed in the TFE just as they dispersed in the water. The dark-bright alternate domains in Fig. 3C and D were ascribed to the formation of birefringent domains. The fingerprint-like pattern in Fig. 3C and a visible banded texture in Fig. 3D are the characteristics of liquid crystal textures (Revel & Marchessaultf, 1993). Thus, chitin nanofibrils can be highly oriented in water and also in TFE with the chitin nanofibril content of as high as 5% (w/v).

It is considered that TFE has a strong ability to form hydrogen-bond due to the high electron-withdrawing ability of the $-CF_3$ group, thus, in TFE suspension the hydrogen-bonds are more easily formed between TFE and chitin nanofibril instead of chitin nanofibrils, which helps to avoid the conglomeration of chitin nanofibrils. Furthermore, a weak acidity nature of TFE can better maintain the positive charge ($NH_3^+$) on chitin nanofibrils' surface, therefore, the electrostatic repulsion of interparticles is also a reason to explain the good dispersion.

### 3.3. Preparation and characterization of n-chitin/PCL nanocomposites

In order to reduce the intensity and time of ultrasonic treatment, we adopted a mild procedure, i.e., adding a solvent-exchange step, to disperse chitin nanofibrils in TFE (see Section 2) and ultimately obtained a better colloidal chitin nanofibril/TFE suspension with a higher solid content to blend with PCL solution. Fig. 4A shows the micrograph of the cross section of n-chitin/PCL film. The bright dots or lines were designated as chitin nanofibrils, which were uniformly dispersed in the PCL matrix; the holes or ditches were ascribed to the imprints of chitin nanofibrils left during cryo-fracturing. The arrows in the photograph pointed that there was an evident gap around a single chitin nanofibril, denoting the adhesion between chitin nanofibril and PCL was relatively weak. The FTIR spectrum also testified the affinity between chitin nanofibril and PCL was weak, since there were no significant changes of the characteristic peak of ester group in n-chitin/PCL film compared to neat PCL film (Fig. S3, Supporting Information). Thus, the chitin nanofibril could be pulled out during cryo-fracturing and left its imprint in the section. The micrograph also shows an evidence of the presence of interconnection between chitin nanofibrils (see circled area), suggesting it was possible that chitin nanofibrils could form three-dimensional percolation structure to reinforce PCL. This point would be confirmed by DMA results in the latter section. The micrograph of the electrospun n-chitin/PCL fiber mat in Fig. 4B revealed the fiber diameter ranged from 200 to 400 nm, and the fiber surface were smooth and without protruding segments of chitin nanofibrils. Thus, chitin nanofibrils presumably located within the fibers. The alignment of chitin nanofibrils was further probed using TEM (Fig. 4C). The dark lines, in the direction parallel to the fiber axis, corresponded to chitin nanofibrils which were easier

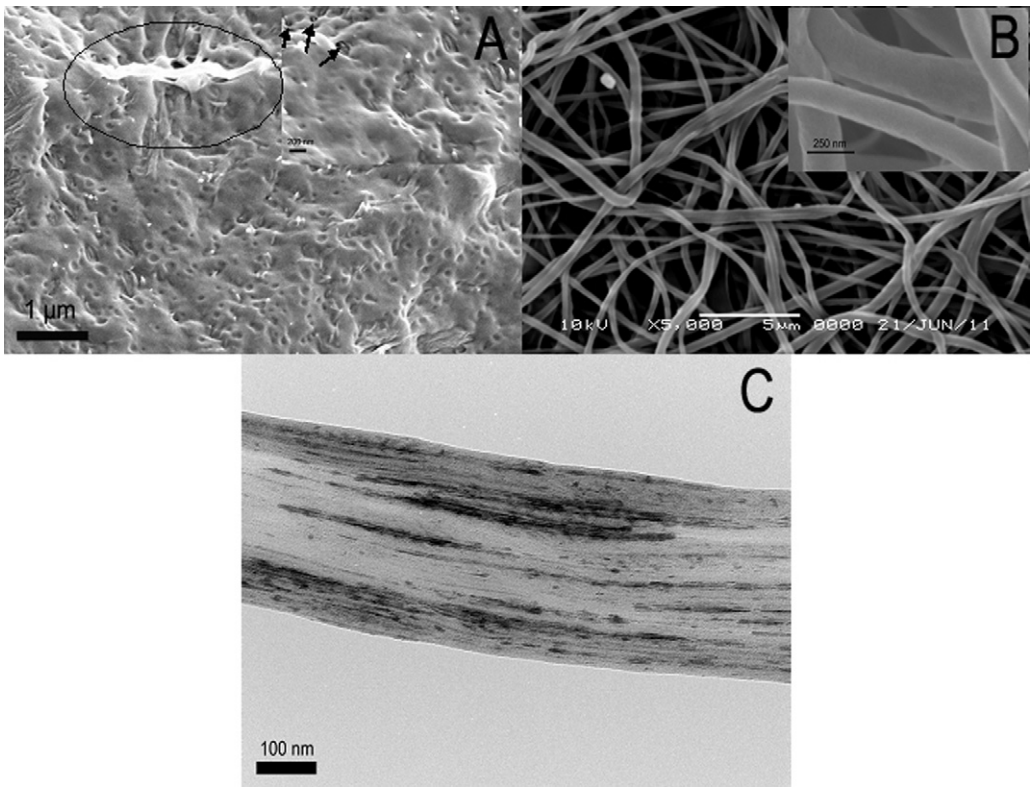


**Fig. 4.** (A) Scanning electron microscopy micrograph of the cross section of n-chitin/PCL film (15:85) and (B) n-chitin/PCL fiber mat (20:80). (C) Transmission electron micrograph of an individual electrospun fiber of n-chitin/PCL fiber mat (20:80). Inset is a higher magnification.

to be electronically stained by uranyl acetate, suggesting that the chitin nanofibrils were embedded within the fibers in the direction parallel to the fiber axis.

To elucidate how chitin nanofibrils were organized in the nanocomposites, DMA was performed both for n-chitin/PCL film and fiber mat. Fig. 5 displays the plots of storage tensile modulus E′ (Fig. 5A) and loss angle tangent tan $\delta$ (Fig. 5B) as a function of temperature for the n-chitin/PCL (20:80) nanocomposite film and fiber mat. At low temperature, the initial tensile modulus of film was much higher than that of fiber mat due to its compact structure. A mild modulus drop appeared for both samples around −54 °C, i.e., in the glass-rubber transition zone, following by a rubbery plateau region. This small modulus drop, in other words, the larger rubbery modulus possibly resulted from the higher degree of crystallinity of the matrix in that the crystalline regions can act as physical crosslinks so as to increase the modulus substantially. The second modulus drop appeared around the melt point of PCL. After this sharp modulus drop, another modulus plateau region occurred both for the film and fiber mat. Since the matrix becomes viscous at $T_m$, this phenomenon implied a stable rigid phase existed in the matrix, i.e., a rigid chitin nanofibril structure. However, the arrangements of chitin nanofibrils in the film and in the fiber mat were different. Thereby, the film and the fiber mat behaved differently after $T_m$. As for film, the rough modulus plateau region with a tendency to decline extended to 300 °C, suggesting chitin nanofibrils form a rigid network in the matrix due to their mutual interactions. As for fiber mat, the modulus remained constant from $T_m$ to 82 °C, subsequently, a third modulus drop appeared. It was considered that the chitin nanofibrils possibly located within fibers and arranged along the fiber long axis; when the PCL matrix melted, the rigid chitin nanofibrils could be as fiber's framework to keep modulus stable to a certain degree; however, the chitin nanofibrils lying in different fibers could not form a network structure due to 'disconnect' and also they could not rearrange to a network within the viscous matrix, therefore, the modulus sharply dropped again at 82 °C. Fig. 5B displays two peaks (see arrows), which were directly linked to these two sharp modulus drops for the fiber mat.

Fig. 6 depicts the uniaxial tensile results of n-chitin/PCL films (A) and fiber mats (B). Here we used a relatively high tensile speed of 100 mm min$^{-1}$, because the samples could not be stretched to break with frequently used speed, i.e., 10 mm min$^{-1}$. The n-chitin/PCL films exhibited a typical type of thermoplastic with a distinct yield point. With the increase of chitin nanofibril content, the yield stress increased gradually from 13 Mpa (5:95) to 21 MPa (30:70), the modulus also greatly increased compared to PCL (200 MPa), the highest being 500 MPa (20:80). However, the increase of peak stress was indistinctive, from 18 Mpa (5:95) to 25 MPa (30:70) compared to PCL (22 Mpa), while the strain at break of all nanocompostites decreased to the range of 400–500% compared to PCL (700%). As for n-chitin/PCL fiber mats, the strain–stress curves exhibited a different type. There were no distinct yield points compared to films. The n-chitin/PCL fiber mats displayed a hard-tough characteristic, while the PCL fiber mat exhibited a soft-tough characteristic. Similarly, with the increase of chitin nanofibril content, the peak stress greatly increased from 11 MPa (5:95) to 18 MPa (30:70) compare to PCL (4 MPa), the modulus also highly increased compared to PCL (12 MPa), the highest being 19 MPa (15:85), however, the strain at break decreased to the range of 250–350% compared to the PCL (680%). In conclusion, the n-chitin/PCL nanocomposite could be obtained directly from non-aqueous medium and the preliminary results showed the chitin nanofibril was a good reinforcing filler to PCL matrix. Our future work will consist of further experiments focusing on the reinforcing mechanisms in both cases of solvent-cast films and electrospun fiber mats.

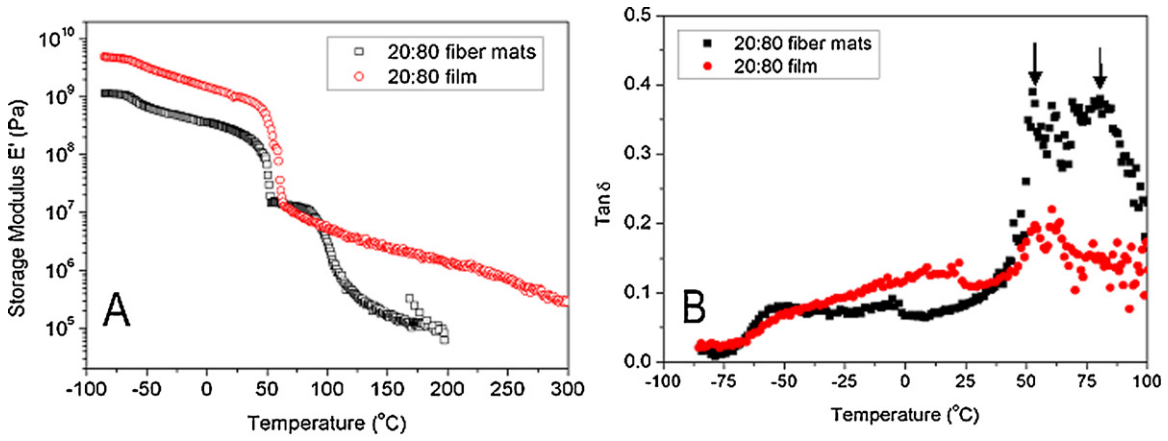


**Fig. 5.** (A) The storage tensile modulus E′ and (B) loss angle tangent tan $\delta$ vs. temperature at 1 Hz for n-chitin/PCL film (20:80) and n-chitin/PCL fiber mat (20:80).

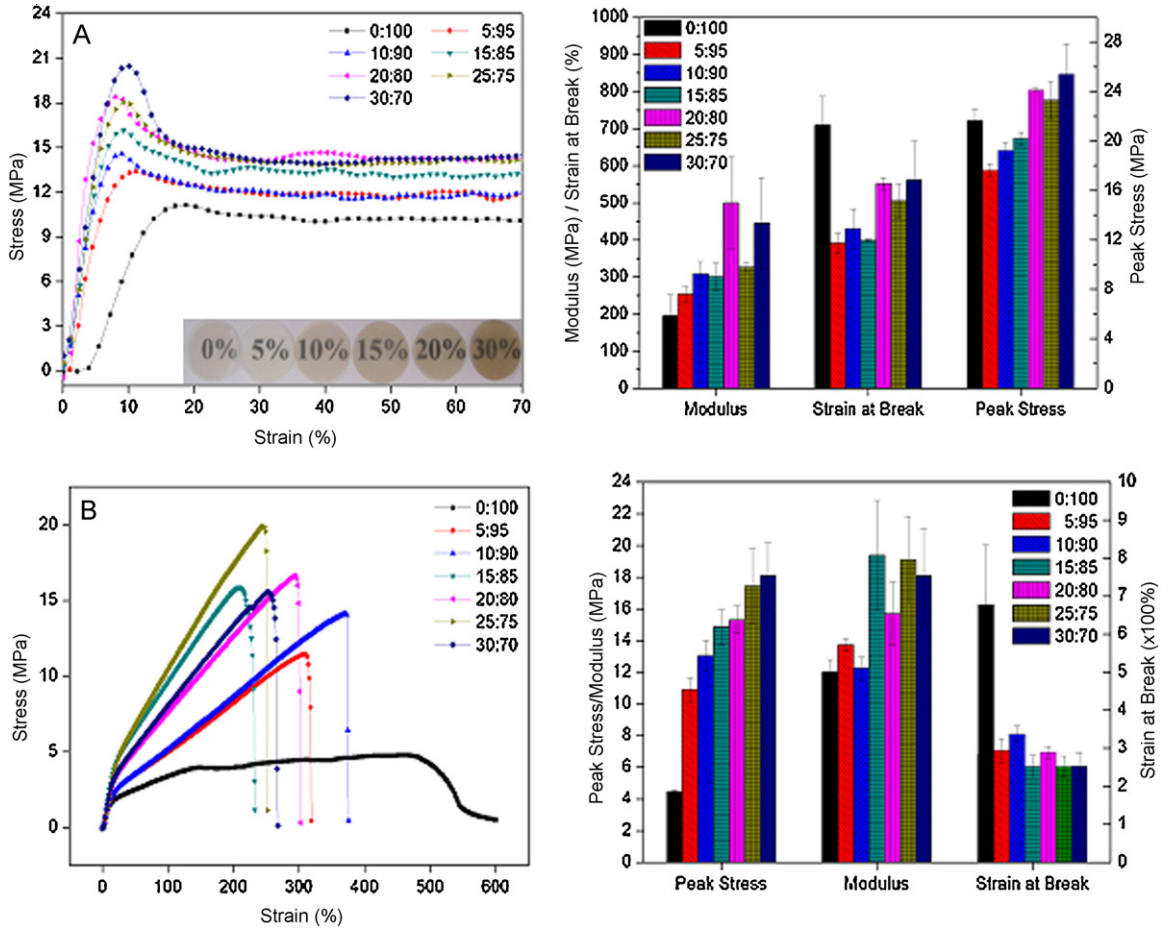


**Fig. 6.** Uniaxial tensile tests of n-chitin/PCL films (A) and n-chitin/PCL fiber mats (B). The strain–stress curve with the highest peak stress from five measurements was selected to display here; the data of peak stress, modulus and strain at break were the average of five measurements. Inset is the pictures of the corresponding nanocomposite films.

## 4. Conclusion

The chitin nanofibril is a good reinforcing filler for biopolymers, but until now, its water related dispersivity restricts its applications. In this paper, it was found that chitin nanofibril could be well dispersed in an organic solvent of TFE, which is also a good solvent for many water-soluble or water-insoluble polymers. Thus, using chitin nanofibril/TFE suspension instead of chitin nanofibril aqueous suspension is a good alternative to broaden the family of chitin nanofibril-based nanocomposites, specifically for the applications in electrospinning tissue engineering scaffolds. Here, the n-chitin/PCL nanocomposites were preliminarily prepared both by solvent-cast approach and electrospinning technique, and their mechanical properties were briefly discussed. It was confirmed that chitin nanofibril was a good reinforcing filler to PCL matrix, although the reinforcing mechanisms in both cases of cast films and fiber mats needs to be further studied.

## Acknowledgements

We appreciate Dr. Kenneth J. Wynne provided DMA measurement. This work was partially supported by the program from the Natural Science Foundation of Shanghai (Grant No. 10ZR1400900).

## Appendix A. Supplementary data

Supplementary data associated with this article can be found, in the online version, at doi:10.1016/j.carbpol.2011.10.066.

## References

Cardenas, G., Cabrera, G., Taboada, E. & Miranda, S. P. (2004). Chitin characterization by SEM, FTIR, XRD, and 13C cross polarization/mass angle spinning NMR. *Journal of Applied Polymer Science*, *93*, 1876–1885.

Carr, M. E., Jr. & Hermans, J. (1978). Size and density of fibrin fibers from turbidity. *Macromolecules*, *11*, 46–50.

Fan, Y., Saito, T. & Isogai, A. (2008). Chitin nanocrystals prepared by TEMPO-mediated oxidation of α-chitin. *Biomacromolecules*, *9*, 192–198.

Feng, L., Zhou, Z., Dufresne, A., Huang, J., Wei, M. & An, L. (2009). Structure and properties of new thermoforming bionanocomposites based on chitin whisker-graft-polycaprolactone. *Journal of Applied Polymer Science*, *112*, 2830–2837.

Gaill, F., Persson, J., Sugiyama, J., Vuong, R. & Chanzy, H. (1992). The chitin system in the tubes of deep sea hydrothermal vent worms. *Journal of Structural Biology*, *109*, 116–128.

Hariraksapitak, P. & Supaphol, P. (2010). Preparation and properties of a-chitin-whisker-reinforced hyaluronan-gelatin nanocomposite scaffolds. *Journal of Applied Polymer Science*, *117*, 3406–3418.

Ifuku, S., Nogi, M., Abe, K., Yoshioka, M., Morimoto, M., Saimoto, H., et al. (2009). Preparation of chitin nanofibers with a uniform width as alpha-chitin from crab shells. *Biomacromolecules*, *10*, 1584–1588.

Ifuku, S., Nogi, M., Yoshioka, M., Morimoto, M., Yano, H. & Saimoto, H. (2010). Fibrillation of dried chitin into 10–20 nm nanofibers by a simple grinding method under acidic conditions. *Carbohydrate Polymers*, *81*, 134–139.

Junkasem, J., Rujiravanit, R., Grady, B. P. & Supaphol, P. (2010). X-ray diffraction and dynamic mechanical analyses of α-chitin whisker-reinforced poly(vinyl alcohol) nanocomposite nanofibers. *Polymer International*, *59*, 85–91.

Kadokawa, J., Takegawa, A., Mine, S. & Prasad, K. (2011). Preparation of chitin nanowhiskers using an ionic liquid and their composite materials with poly(vinyl alcohol). *Carbohydrate Polymers*, *84*, 1408–1412.

Lu, Y., Weng, L. & Zhang, L. (2004). Morphology and properties of soy protein isolate thermoplastics reinforced with chitin whiskers. *Biomacromolecules*, *5*, 1046–1051.

Mathew, A. P., Laborie, M. G. & Oksman, K. (2009). Cross-linked chitosan/chitin crystal nanocomposites with improved permeation selectivity and pH stability. *Biomacromolecules*, *10*, 1627–1632.

Muzzarelli, R. A. A., Morganti, P., Morganti, G., Palombo, P., Palombo, M., Biagini, G., et al. (2007). Chitin nanofibrils/chitosan glycolate composites as wound medicaments. *Carbohydrate Polymers*, *70*, 274–284.

Muzzarelli, R. A. A. (2011a). Biomedical exploitation of chitin and chitosan via mechano-chemical disassembly, electrospinning, dissolution in imidazolium ionic liquids, and supercritical drying. *Marine Drugs*, *9*, 1510–1533.

Muzzarelli, R. A. A. (2011b). New techniques for optimization of surface area and porosity in nanochitins and nanochitosans. *Advances in Polymer Science*, *247*, 167–186.

Muzzarelli, R. A. A. (2011c). Nanochitins and nanochitosans, paving the way to eco-friendly and energy-saving exploitation of marine resources. In J. McGrath, & R. Hoefer (Eds.), *Comprehensive polymer science: Polymers for sustainable environment and energy*. Heidelberg: Springer.

Muzzarelli, R. A. A. (2011d). Chitin nanostructures in living organisms. In S. N. Gupta (Ed.), *Chitin formation and diagenesis*. New York: Springer.

Nair, K. G. & Dufresne, A. (2003). Crab shell chitin whisker reinforced natural rubber nanocomposites. 1. Processing and swelling behavior. *Biomacromolecules*, *4*, 657–665.

Okita, Y., Fujisawa, S., Saito, T. & Isoga, A. (2011). TEMPO-oxidized cellulose nanofibrils dispersed in organic solvents. *Biomacromolecules*, *12*, 518–522.

Paillet, M. & Dufresne, A. (2001). Chitin whisker reinforced thermoplastic nanocomposites. *Macromolecules*, *34*, 6527–6530.

Revel, J. F. & Marchessaultf, R. H. (1993). In-vitro chiral nematic ordering of chitin crystallites. *International Journal of Biological Macromolecules*, *15*, 329–335.

Sannan, T., Kurita, K., Ogura, K. & Iwakura, Y. (1978). Studies on chitin. 7. I.r. spectroscopic determination of degree of deacetylation. *Polymer*, *19*, 458–459.

Shalumon, K. T., Anulekha, K. H., Chennazhi, K. P., Tamura, H., Nair, S. V. & Jayakumar, R. (2011). Fabrication of chitosan/poly(caprolactone) nanofibrous scaffold for bone and skin tissue engineering. *International Journal of Biological Macromolecules*, *48*, 571–576.

Sriupayo, J., Supaphol, P., Blackwell, J. & Rujiravanit, R. (2005a). Preparation and characterization of a-chitin whisker-reinforced chitosan nanocomposite films with or without heat treatment. *Carbohydrate Polymers*, *62*, 130–136.

Sriupayo, J., Supaphol, P., Blackwell, J. & Rujiravanit, R. (2005b). Preparation and characterization of a-chitin whisker-reinforced poly(vinyl alcohol) nanocomposite films with or without heat treatment. *Polymer*, *46*, 5637–5644.

Watthanaphanit, A., Supaphol, P., Tamura, H., Tokura, S. & Rujiravanit, R. (2008). Fabrication, structure, and properties of chitin whisker-reinforced alginate nanocomposite fibers. *Journal of Applied Polymer Science*, *110*, 890–899.

Wongpanit, P., Sanchavanakit, N., Pavasant, P., Bunaprasert, T., Tabata, Y. & Rujiravanit, R. (2007). Preparation and characterization of chitin whisker-reinforced silk fibroin nanocomposite sponges. *European Polymer Journal*, *43*, 4123–4135.

Zengab, M., Gaoa, H., Wua, Y., Fana, L. & Li, A. (2010). Preparation and characterization of nanocomposite films from chitin whisker and waterborne poly(ester-urethane) with or without ultra-sonification treatment. *Journal of Macromolecular Science, Part A*, *47*, 867–876.